CORROSION SCIENCE AND TECHNOLOGY, Vol.22, No.6(2023), pp.393~398 pISSN 1598-6462 / eISSN 2288-6524
[Research Paper] DOI: https://doi.org/10.14773/cst.2023.22.6.393

Microstructures and Mechanical Properties of HfN Coatings Deposited by DC, Mid-Frequency, and ICP Magnetron Sputtering

Sung-Yong Chun†

Department of Advanced Materials Science and Engineering, Mokpo National University, Jeonnam 58554, Korea
(Received June 28, 2023; Revised August 22, 2023; Accepted August 23, 2023)

Properties of hafnium nitride (HfN) coatings are affected by deposition conditions, most often by the sputtering technique. Appropriate use of different magnetron sputtering modes allows control of the structural development of the film, thereby enabling adjustment of its properties. This study compared properties of HfN coatings deposited by direct current magnetron sputtering (dcMS), mid-frequency direct current magnetron sputtering (mfMS), and inductively coupled plasma-assisted magnetron sputtering (ICPMS) systems. The microstructure, crystalline, and mechanical properties of these HfN coatings were investigated by field emission electron microscopy, X-ray diffraction, atomic force microscopy, and nanoindentation measurements. HfN coatings deposited using ICPMS showed smooth and highly dense microstructures, whereas those deposited by dcMS showed rough and columnar structures. Crystalline structures of HfN coatings deposited using ICPMS showed a single δ-HfN phase, whereas those deposited using dcMS and mfMS showed a mixed δ-HfN and $HfN_{0.4}$ phases. Their performance were increased in the order of dcMS < mfMS < ICPMS, with ICPMS achieving a value of 47.0 GPa, surpassing previously reported results.

Keywords: *Direct current magnetron sputtering, Mid-frequency magnetron sputtering, Inductively coupled plasma-assisted magnetron sputtering, HfN, Coatings*

1. Introduction

Because hafnium nitride (HfN) coatings have the same rock salt crystal structure as metallic nitrides such as TiN, CrN, and TiAlN, they hold promise for application in electronic devices such as dielectrics, as well as mechanical applications that require wear resistance, and high hardness and elastic modulus [1-3]. The properties of the crystal structure of HfN are reported to be excellent; the δ-HfN crystal phase with a rock-salt structure is usually obtained when the sputtering method is used for fabrication [4]. The literature records various deposition methods for producing HfN coatings, including magnetron sputtering, pulsed laser deposition, and metalorganic chemical vapor deposition. Magnetron sputtering is widely used because of its excellent reproducibility and adhesion, as well as its high deposition rate and low substrate temperature [5–8]. However, when the substrate temperature is lower than room temperature (15 to 25 °C), a microstructure with a columnar structure or a porous coating film is easily produced, which is disadvantageous in applications requiring a high density [9]. Therefore, in this study, we prepared HfN coatings using the following three methods, and compared their properties: direct current magnetron sputtering (dcMS), which is a traditional magnetron sputtering method; mid-frequency magnetron sputtering (mfMS), which has attracted attention because of its ability to control pulse plasma parameters such as the pulse frequency and duty cycle; and, inductively coupled plasma-assisted magnetron sputtering (ICPMS), which can produce coating films with uniform thickness and excellent mechanical properties at a high ion density and low deposition temperature.

In ICPMS, plasma is generated by applying a voltage to a circular coil-shaped antenna using radiofrequency (RF) power. Moreover, energy is easily transferred through the antenna to charged particles in the antenna, which is an inductive element. In contrast to internal electrodes and electron cyclotron resonance, this method does not require the application of a direct-current magnetic field and can be utilized for plasma treatment

†Corresponding author: sychun@mokpo.ac.kr
Sung-Yong Chun: Professor

of relatively large work pieces, making it the focus of considerable research attention [10]. Reports on the preparation of HfN coatings using the traditional dcMS or the radio frequency magnetron sputtering (rfMS) have also recently attracted attention; however, there have been no reports on the preparation of HfN coatings using ICPMS, nor on the comparison of the properties of HfN coatings obtained by these three magnetron-sputtering methods [11-13]. Therefore, in this study, we prepared HfN coatings using three different coating methods: dcMS, mfMS, and ICPMS. Then, we compared the two-dimensional surface and cross-sectional microstructures of the coatings, along with their three-dimensional microstructures, i.e., morphologies. We also compared their structural properties, such as the crystal structure and preferred orientation, and their mechanical and physical properties, such as the nanoindentation hardness and elastic modulus.

2. Experimental Method

In the experiment, a Si (100) substrate was used to fabricate the HfN coatings. The substrate was cleaned in acetone and ethyl alcohol for 10 min per Hf target using an ultrasonic cleaner to remove impurities on the substrate surface and then dried. During the fabrication of the coatings using the three sputtering methods, the experimental conditions were maintained, with the same coating chamber, process atmosphere, and process conditions, for an accurate comparison of the properties. The HfN coatings were fabricated by dcMS, mfMS, and ICPMS by simply changing the magnetron sputtering power. Hf targets with a diameter of 76.2 mm, a thickness of 6.35 mm, and a purity of 99.99% were used as starting materials. For the process atmosphere, we used ultrahigh-purity N_2 and Ar gases and fixed the Ar and N_2 injection rates at 31 and 5 sccm, respectively. A mass flow controller (MFC) was used for the partial pressure control of the Ar and N_2 gases. The distance between the substrate and the target was maintained at 60 mm during deposition, and the substrate was rotated at a speed of approximately 10 rpm for uniform deposition. The chamber was evacuated to an initial pressure of approximately 3.0×10^{-6} Torr using a rotary pump and a turbomolecular pump, and the vacuum level was measured using an ion gauge and a Baratron gauge. Preliminary sputtering was performed in an Ar atmosphere to clean the target and substrate prior to deposition. Three types of HfN coatings were prepared using dcMS, mfMS, and ICPMS. Table 1 presents the coating conditions. A grazing incidence X-ray diffractometer (X'Pert Pro MRD, PANalytical) was used to analyze the crystalline phases and preferred orientations of the HfN coatings. Field-emission scanning electron microscopy (FE-SEM, S-3500N, Hitachi) and atomic force microscopy (AFM, Nanoscope IIIa, Digital Instruments) were used to examine the two- and three-dimensional microstructures and morphologies. A nanoindentator (Nanoindentation Hardness Tester, MTS XP, MTS Systems Corporation)—a precision hardness tester for thin films—was used to precisely measure the mechanical properties of the coatings. The hardness was measured using a Berkovich diamond indenter, and the mean value was calculated for 16 measurements per specimen.

Table 1. Conditions for deposition of HfN coatings using dcMS, mfMS, and ICPMS

Conditions	1	2	3
Sputtering (type)	dcMS	mfMS	ICPMS
Sputtering Power (W)	300	300	300
ICP Power (W)	-	-	200
Pulse frequency (kHz)	-	15	-
Duty cycle (%)	-	85	-
Substrate bias voltage (V)	-100	-100	-100

3. Results and Discussion

HfN coatings were prepared under three deposition conditions using dcMS and ICPMS equipment. Then, their microstructures and mechanical properties, such as their surface and cross-sectional microstructures, three-dimensional morphologies, surface roughness, hardness, and Young's modulus, were analyzed.

3.1 Crystal structure and preferred orientation

Fig. 1 shows the X-ray diffraction analysis results for the HfN coatings prepared by dcMS, mfMS, and ICPMS. As shown in Fig. 1a, for the HfN coatings prepared by dcMS, δ-HfN [111] and $HfN_{0.4}$ [103] crystal peaks were

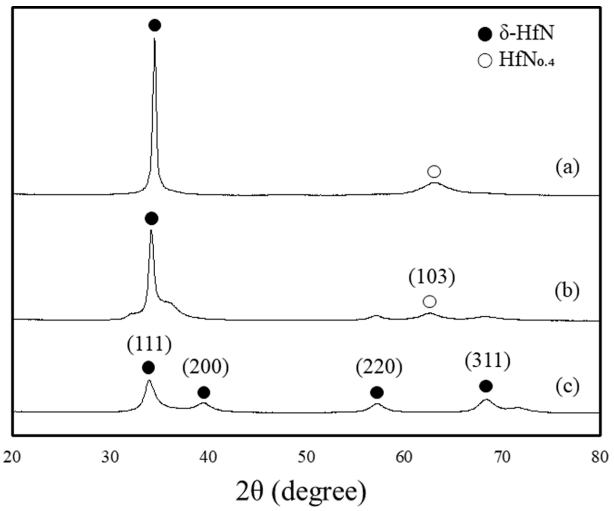

Fig. 1. XRD data of HfN coatings deposited using (a) dcMS, (b) mfMS, and (c) ICPMS

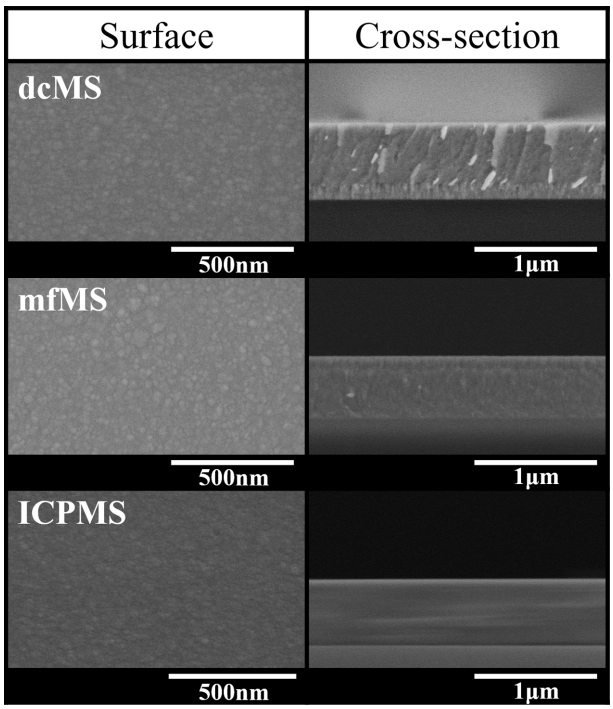

Fig. 2. Surface and cross-sectional FE-SEM images of HfN coatings deposited using dcMS, mfMS, and ICPMS

observed, whereas for the HfN coatings prepared by mfMS, as shown in Fig. 1b, a δ-HfN [111] main peak was observed along with an $HfN_{0.4}$ [103] crystal peak and δ-HfN [220] and δ-HfN [311] peaks that had significantly lower intensities. As shown in Fig. 1c, for the HfN coatings prepared by ICPMS, only δ-HfN [111], [200], [220], [311] crystal peaks were observed, and, in contrast to the cases of (a) and (b), no $HfN_{0.4}$ [103] crystal peak was observed.

3.2 Microstructure

The microstructures of the HfN coatings prepared by dcMS, mfMS, and ICPMS were examined using FE-SEM, and images of their surfaces and cross sections are shown in Fig. 2. For the HfN coatings prepared by dcMS, the surface microstructure indicated a rough surface with pores, and the cross-sectional microstructure exhibited grains with a typical columnar structure from the substrate surface to the film surface. For the HfN coatings prepared by mfMS, the porous columnar structure was absent in the cross section, and the surface was smoother, with significantly finer grains. The HfN coatings prepared by ICPMS had smoother surfaces than those prepared by dcMS and mfMS. Furthermore, the porous columnar structure was absent, as in the case of mfMS, and a dense microstructure was observed from the substrate surface to the film surface. The results indicated that the coating microstructure depended significantly on the magnetron sputtering mode. The HfN coatings prepared by mfMS and ICPMS had denser cross-sectional structures and smoother surfaces than those prepared by the conventional dcMS method. This was due to the generation of dense plasma with a high ionization rate in mfMS and ICPMS, as well as the ion bombardment effect. It is generally accepted that ion bombardment has a significant impact on the densification of the microstructure and can strengthen the adhesion between the substrate and the coating film [14]. In this study, the HfN coatings prepared by ICPMS had denser microstructures than those prepared by mfMS. It is likely that increasing the ICP density increases the kinetic energy of the charged particles entering the substrate, which improves the adatom mobility on the substrate surface, and this reduces the generation of pores during the formation of the coating film, resulting in a denser film.

3.3 Three-dimensional morphology and surface roughness

To compare the effects of dcMS, mfMS, and ICPMS on the three-dimensional morphologies and surface roughness of the HfN coatings, we performed noncontact

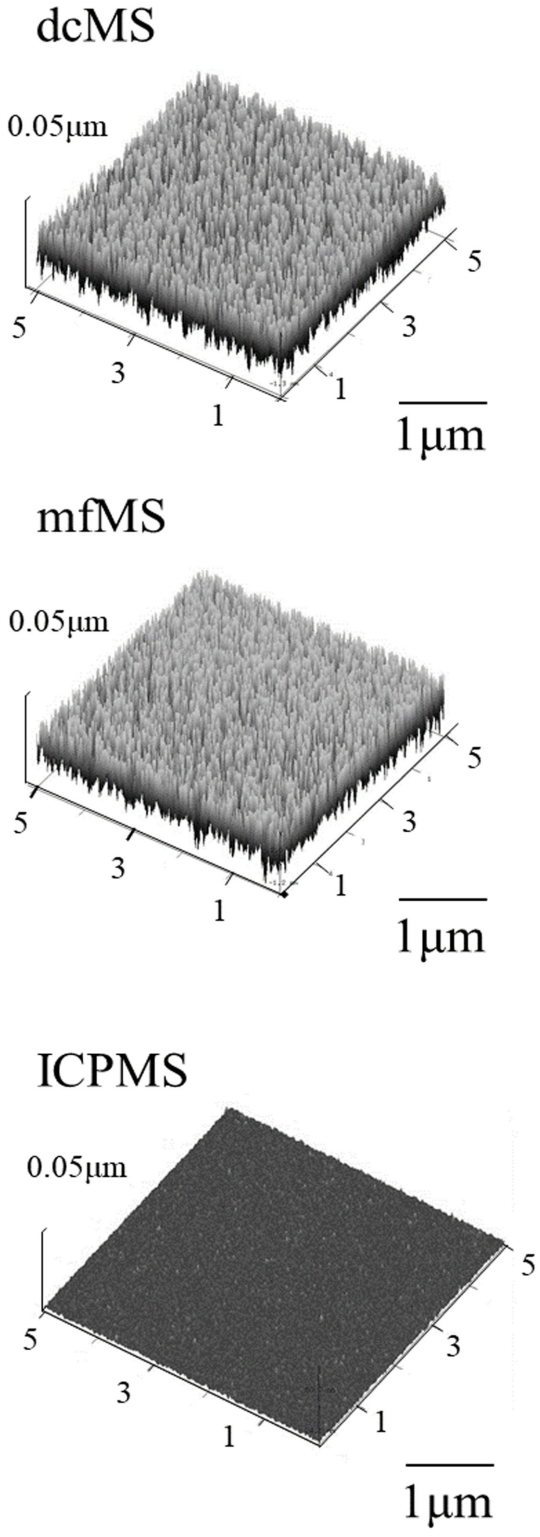

Fig. 3. AFM surface morphologies of HfN coatings deposited using dcMS, mfMS, and ICPMS

AFM, and the results are shown in Fig. 3. Comparing the effects of the three sputtering methods on the surface

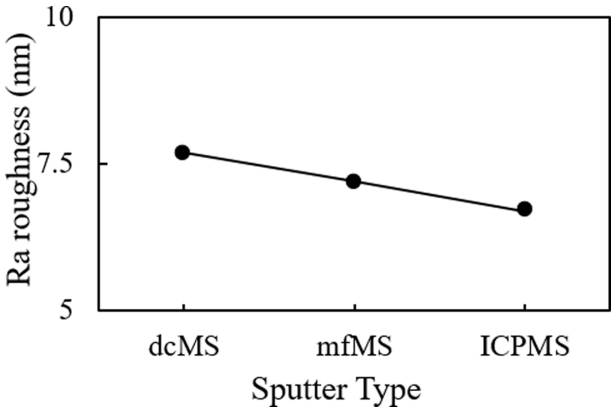

Fig. 4. Ra roughness data of HfN coatings deposited using dcMS, mfMS, and ICPMS

roughness (Ra) of the HfN coatings revealed that the density and flatness of the morphology increased in the following order: dcMS, mfMS, and ICPMS. The formation of a denser and flatter morphology and finer grains in the HfN coatings prepared by mfMS and ICPMS is attributed to two main factors: 1) the ion bombardment effect of accelerated ions due to the increase in ion energy and 2) the increase in nucleation density [15]. Fig. 4 shows the surface roughness (Ra) of the HfN coatings, which was 7.7, 7.2, and 6.7 nm for coatings prepared by dcMS, mfMS, and ICPMS, respectively. It can be seen that the Ra value decreased in the order of dcMS, mfMS, and ICPMS. These results can be explained as follows: the ICPMS method has a plasma density approximately 1000 times higher than the conventional dcMS method, a higher metal ion fraction of the target material in the plasma, and a lower process pressure, resulting in a finer coating structure [16]. T. H. Kim *et al.* [17] compared the measured plasma densities between dcMS and ICPMS. The plasma density in the dcMS method was $10^{9}\,cm^{-3}$, and that in the ICPMS method was $10^{12}\,cm^{-3}$, corresponding to a 1000-fold difference [17].

3.4 Nanoindentation hardness and Young's modulus

The hardness measurement of thin-coating films with a thickness of tens to hundreds of nanometers is impossible with conventional micro-Vickers hardness testers. Furthermore, precise measurement is difficult owing to the nanoindentation size effect. Thus, for precise hardness measurement of coating films with a thickness of $< 1\,\mu m$, the use of nanoindentation hardness-

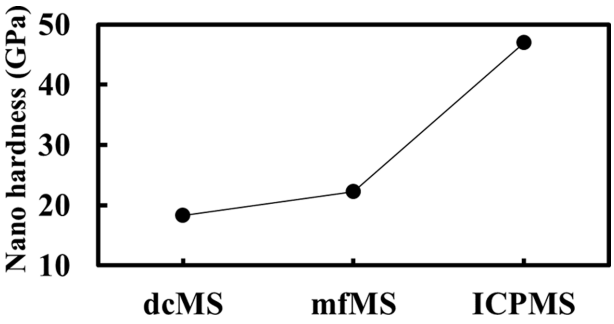

Fig. 5. Nanoindentation hardness of HfN coatings deposited using dcMS, mfMS, and ICPMS

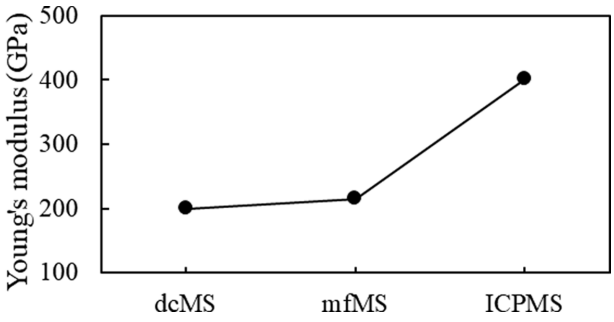

Fig. 6. Young's modulus of HfN coatings deposited using dcMS, mfMS, and ICPMS

measurement equipment is desirable. To exclude the indentation size effect, which tends to increase the measured hardness value as the indentation depth decreases, the measurement positions were averaged to the 1/10 position of the total film thickness. The nanoindentation hardness and elastic modulus (Young's modulus) measurement results for the HfN coatings prepared by dcMS, mfMS, and ICPMS obtained in this manner are depicted in Fig.s 5 and 6. As shown in Fig. 5, the nanoindentation hardness of the HfN coatings prepared by ICPMS was higher than that of the coatings prepared by dcMS and mfMS. The nanoindentation hardness of the HfN coatings prepared by dcMS and mfMS was 18.3 and 22.3 GPa, respectively, whereas that of the HfN coatings prepared by ICPMS was 47.0 GPa, approximately 2.6 times higher than the value for the dcMS method. It is noteworthy that this nanoindentation hardness (ICPMS) is far superior to those in all previously reported results for HfN coatings. As shown in Fig. 6, the HfN coatings prepared by ICPMS had the highest Young's modulus: 401.0 GPa. The Young's moduli of the HfN coatings prepared by dcMS and mfMS were 199.9 and 215.0 GPa, respectively. Thus, the Young's modulus increased in the order of dcMS, mfMS, and ICPMS, similar to the nanoindentation results shown in Fig. 5. This improvement in mechanical properties is attributed to the phase change of the HfN coating film and the grain-size reduction [18,19].

4. Conclusion

In this study, HfN coatings were prepared by three different magnetron sputtering methods —dcMS, mfMS, and ICPMS—and their structural and mechanical properties were compared. The magnetron sputtering mode affected the refinement of coating grains, the surface and cross-sectional microstructures, and the crystallographic properties, such as the crystal structure and preferred orientation. In the X-ray diffraction spectra, $HfN_{0.4}$ [103] and δ-HfN [111] peaks were observed for the HfN coatings prepared by dcMS and mfMS, but only single-phase δ-HfN [111], [200], [220], and [311] peaks were observed for the HfN coatings prepared by ICPMS. In the HfN coatings with a rough surface and columnar structure, the columnar structure disappeared when the sputtering mode changed from the dcMS method to the mfMS and ICPMS methods, and the microstructure changed to a dense and flat surface. The nanoindentation hardness of the HfN coatings prepared by dcMS and mfMS was 18.3 and 22.3 GPa, respectively, and that for the ICPMS method was 47.0 GPa, which is far better than all previously reported results.

Acknowledgments

This work was supported by the National Research Foundation of Korea (NRF) grant funded by the Korea government (MSIT). (No. 2022H1D8A303867111)

References

1. S. Y. Chun, J. Y. Hwang, Effects of Duty Cycle and Pulse Frequency on the Microstructure and Mechanical Properties of TiAlN Coatings, *Journal of The Korean Ceramic Society*, **51,** 447 (2014). Doi: https://doi.org/10.4191/kcers.2014.51.5.447

2. S. Y. Chun, S. J. Kim, Enhancement of the Corrosion Resistance of CrN Film Deposited by Inductively Coupled Plasma Magnetron Sputtering, *Corrosion Science and Technology*, **20**, 112 (2021). Doi: https://doi.org/10.14773/cst.2021.20.3.112
3. S. Y. Chun, Microstructure and Mechanical Properties of Nanocrystalline TiN Films Through Increasing Substrate Bias, *Journal of the Korean Ceramic Society*, **47**, 479 (2010). Doi: https://doi.org/10.4191/kcers.2010.47.6.479
4. Y. S. Fang, K. A. Chiu, H. Do, L. Chang, Reactive sputtering for highly oriented HfN film growth on Si (100) substrate, *Surface and Coatings Technology*, **377**, 124877 (2019). Doi: https://doi.org/10.3390/coatings10070647
5. R. Armitage, Q. Yang, H. Feick, J. Gebauer, E.R. Weber, Lattice-matched HfN buffer layers for epitaxy of GaN on Si, *Journal of Applied Physics*, **81**, 1450 (2002). Doi: https://doi.org/10.1063/1.1501447
6. J. J. Oakes, A comparative evaluation of HfN, Al2O3, TiC and TiN coatings on cemented carbide tools, *Thin Solid Films*, **107**, 159-165 (1983). Doi: https://doi.org/10.1016/0040-6090(83)90018-4
7. X. M. Cai, F. Ye, E. Q. Xie, D. P. Zhang, P. Fan, Field electron emission from HfNxOythin films deposited by direct current sputtering, *Applied Surface Science*, **254**, 3074 (2008). Doi: https://doi.org/10.1016/j.apsusc.2007.10.058
8. I. E. Fragkos, N. Tansu, Surface plasmon coupling in GaN:Eu light emitters with metal-nitrides, *Scientific Reports*, **8**, 13365 (2018). Doi: https://doi.org/10.1038/s41598-018-31821-8
9. S. Y. Tan, X. H. Zhang, X. J. Wu, F. Fang, J. Q. Jiang, Comparison of chromium nitride coatings deposited by DC and RF magnetron sputtering, *Thin Solid Films*, **519**, 2116 (2011). Doi: https://doi.org/10.1016/j.tsf.2010.10.067
10. F. Ge, P. Zhu, F. Meng, Q. Xue and F. Huang, Achieving Very Low Wear Rates in Binary Transition-Metal Nitrides: The Case of Magnetron Sputtered Dense and Highly Oriented VN Coatings, *Surface and Coatings Technology*, **248**, 81 (2014). Doi: https://doi.org/10.1016/j.surfcoat.2014.03.035
11. R. Nowak, S. Maruno, Surface deformation and electrical properties of HfN thin films deposited by reactive sputtering, *Materials Science and Engineering: A*, **202**, 226 (1995). Doi: https://doi.org/10.1016/0921-5093(95)09814-3
12. S. Y. Chun, Mechanical and Structural Behaviors of HfN Thin Films Fabricated by Direct Current and Mid-frequency Magnetron Sputtering, *Corrosion Science and Technology*, **22**, 30 (2023). Doi: https://doi.org/10.14773/cst.2023.22.1.30
13. C. Escobar, M. Villarreal, J. C. Caicedo, W. Aperador, P. Prieto, Novel performance in physical and corrosion resistance HfN/VN coating system, *Surface and Coatings Technology*, **221**, 182 (2013). Doi: https://doi.org/10.1016/j.surfcoat.2013.02.002
14. I. Petrov, L. Hultman, U. Helmersson, S. A. Barnett, J. E. Sundgern, J. E. Green, Microstructure modification of TiN by ion bombardment during reactive sputter deposition, *Thin Solid Films*, **169**, 299 (1989). Doi: https://doi.org/10.1016/0040-6090(89)90713-X
15. S. Y. Chun, D. H. Seo, Growth Behavior of Nanocrystalline CrN Coatings by Inductively Coupled Plasma (ICP) Assisted Magnetron Sputtering, *Journal of The Korean Ceramic Society*, **49**, 556 (2012). Doi: https://doi.org/10.4191/kcers.2012.49.6.556
16. J. J. Lee, J. H. Joo, Application of inductively coupled plasma to super-hard and decorative coatings, *Surface and Coatings Technology*, **169-170**, 353 (2003). Doi: https://doi.org/10.1016/S0257-8972(03)00112-9
17. T. H. Kim, G. Y. Yeom, A Review of Inductively Coupled Plasma-Assisted Magnetron Sputter System, *Applied Science and Convergence Technology*, **28**, 131 (2019). Doi: https://doi.org/10.5757/ASCT.2019.28.5.131
18. C. Rebholz, A. Leyland, A. Matthews, C. Charitidis, S. Logothetidis, D. Schneider, Correlation of elastic modulus, hardness and density for sputtered TiAlBN thin films, *Thin Solid Films*, **514**, 81 (2006). Doi: https://doi.org/10.1016/j.tsf.2006.02.038
19. F. Zhu, K. Zhu, Y. Hu, Y. Ling, D. Wang, H. Peng, Z. Xie, R. Yang, Z. Zhang, Microstructure and Young's modulus of ZrN thin film prepared by dual ion beam sputtering deposition, *Surface and Coatings Technology*, **374**, 997 (2019). Doi: https://doi.org/10.1016/j.surfcoat.2019.06.094